High-Pressure Stopped-Flow Polymerization for Polypropene-*block*-poly(ethene-*co*-propene) Having Controlled Molecular Weight: Synthesis and Characterization

Hideharu Mori,[†] Mikio Yamahiro,[†] Valery V. Prokhorov,[‡] Koh-hei Nitta,[‡] and Minoru Terano*[,†]

School of Materials Science and Center for New Materials, Japan Advanced Institute of Science and Technology, Asahidai 1−1, Tatsunokuchi, Ishikawa 923-1292, Japan

Received November 30, 1998

ABSTRACT: A high-pressure-type stopped-flow polymerization system was developed for the production of a real block copolymer, polypropene-*block*-poly(ethene-*co*-propene), having a variable molecular weight. The preliminary homopolymerization experiments of propene at 1−6 atm for 0.1 s with an $MgCl_2$-supported Ziegler catalyst and TEA indicated that the polymer yield and molecular weight of the resulting polypropene were proportional to the monomer concentration in the system. This indicates that the catalyst activity is constant and the unfavorable side reactions can be negligible, i.e., independent of the monomer pressure. The higher propene and ethene concentrations, which could be regulated by the pressures of the vessels in the apparatus, were found to induce a higher molecular weight of the resulting block copolymer without a significant change in the molecular weight distribution and microstructure. The CFC, DSC, and AFM analyses results indicated that the increased molecular weight had an influence only on the lamellar thickness but had no effect on the crystallinity and its distribution of the block copolymer.

Introduction

The synthesis of well-defined polymers and copolymers with predetermined molecular weights and chain topologies is one of the ultimate targets of preparative polymer chemistry. However, the precise control of olefin polymerization with a conventional heterogeneous Ziegler−Natta catalyst has been considered difficult for a long time because of inevitable side reactions, such as catalyst deactivation and various transfer reactions.[1−5] The unfavorable side reactions and short-lived growing polymer chain are also the main reasons for the difficult synthesis of a real olefin block copolymer having a chemical linkage between two different segments.

Under this situation, we successfully developed the modified stopped-flow polymerization method, by which a reaction can be conducted within an extremely short period, for the synthesis of a novel olefin block copolymer, polypropene-*block*-poly(ethene-*co*-propene) [PP-*b*-(PE-*co*-PP)].[6] The stopped-flow polymerization was performed within about 0.2 s, which is shorter than the lifetime of the growing chain. The activity of the catalyst was constant without deactivation in the region. Characterization of the resulting block copolymer was conducted using the various methods, such as ^{13}C NMR spectroscopy, cross fractionation chromatography, differential scanning calorimetry, transmission electron microscopy, dynamic mechanical analysis.[6−9] These results consistently indicated the existence of a chemical linkage between the crystalline polypropene (PP) and amorphous poly(ethene-*co*-propene) (PE-*co*-PP). The effect of the addition of PP-*b*-(PE-*co*-PP) to PP/PE-*co*-PP blends was also confirmed in terms of the mechanical properties.[10,11] The regulation of the composition of each block part was achieved by changing the polymerization times.[6−8] The improvement of the stereoregularity of the PP part in the block copolymer was also attained by using suitable electron donors.[9] Hence, these methods enable us to control the microstructure of PP-*b*-(PE-*co*-PP) by choosing suitable polymerization conditions. This study deals with the regulation of the molecular weight of the PP-*b*-(PE-*co*-PP) by changing monomer pressures in the system.

Many studies concerning the influence of molecular weight on the various properties of polyolefins have been performed due to its scientific interest and industrial importance.[12−14] As for the PP homopolymers, the main structural factors affecting the end-use properties, such as good rigidity and high thermal resistance, are isotacticity and molecular weight and distribution, mostly through their influence on crystallinity. Among them, molecular weight is a strong contributor to the definition of properties as follows:[12] A low molecular weight has a positive effect on crystallinity by allowing the chains to rearrange more rapidly and thus create more perfect crystals. More significant than the crystallinity effect, a lower molecular weight inserts more chain ends into the structure, resulting in fewer chains completely integrated into the crystal to sustain stress during tensile loading, causing failure at elongation in both tensile and impact tests. The drastic drop in the impact strength arises with decreasing molecular weight in homopolymers and even in impact copolymers. In injection molded parts, higher molecular weight polymers cause significant increases in the amount of orientation that results from normal melt processing. Therefore, the regulation of the molecular weight is considered to be a key technology to obtain a high-performance novel olefin block polymer.

* To whom correspondence should be addressed. Telephone: +81 761 51 1620. Fax: +81 761 51 1625. E-mail: terano@jaist.ac.jp.
[†] School of Materials Science.
[‡] Center for New Materials.

10.1021/ma981862b CCC: $18.00
Published on Web 08/31/1999

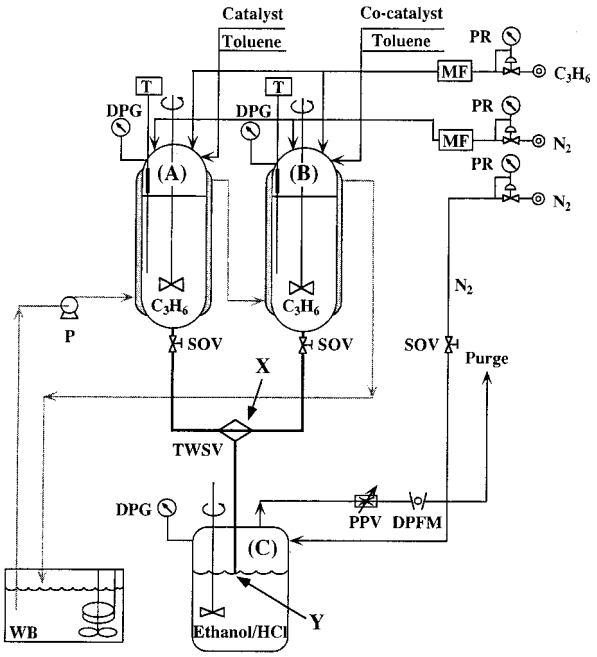

Figure 1. Schematic illustration of high-pressure-type stopped-flow polymerization apparatus for the propene homopolymerization: catalyst slurry in propene-saturated toluene (A), $Al(C_2H_5)_3$ solution in propene-saturated toluene (B), ethanol with HCl (pressure preservation tank, C), three-way stainless-steel valve (TWSV, X), digital pressure gauge (DPG), shut off valve (SOV), mass-flow controller (MF), digital thermometer (T), pressure regulator (PR), digital purge flow meter (DPFM), pressure preservation valve (PPV), pump (P), water bath (WB).

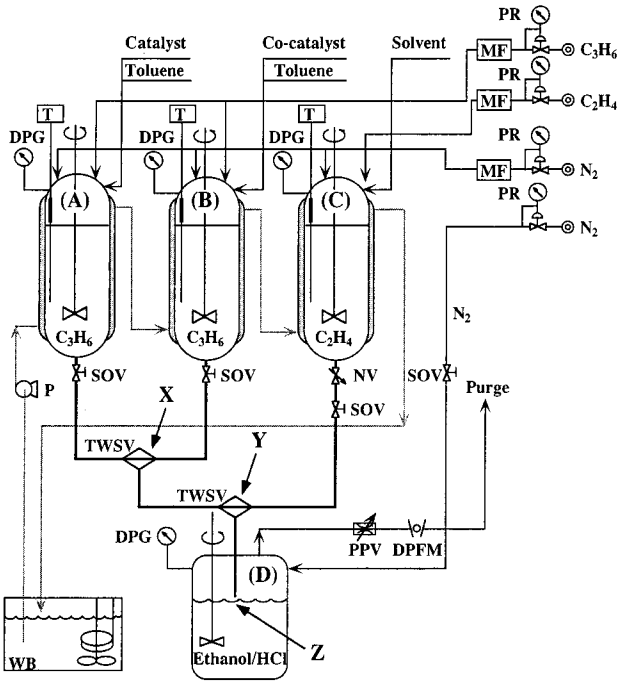

Figure 2. Schematic illustration of high-pressure-type stopped-flow polymerization apparatus for the synthesis of block copolymer: catalyst slurry in propene-saturated toluene (A), $Al(C_2H_5)_3$ solution in propene-saturated toluene (B), ethene-saturated toluene (C), ethanol with HCl (pressure preservation tank, D), needle valve (NV). Other abbreviations are the same as those in Figure 1.

In this study, a high-pressure-type stopped-flow polymerization system was developed as a part of our program of investigating an olefin block copolymer with a well-defined structure and excellent properties. Higher monomer pressures are expected to accelerate the polymerization in order to achieve a PP-*b*-(PE-*co*-PP) having a higher molecular weight. The influence of the monomer pressures, namely, the monomer concentrations in the system, on the polymer yield and molecular weight and the microstructure of the resulting block copolymer was investigated using the technique. The correlation of the molecular weight to the crystalline morphology and supermolecular structure of the block copolymer was investigated by using modern techniques.

Experimental Section

Catalyst and Materials. The highly active $MgCl_2$-supported Ziegler catalyst ($TiCl_4$/ethyl benzoate/$MgCl_2$) used in this study was prepared according to a previously reported method.[6] The catalyst was used as a toluene slurry, and the Ti content of the catalyst was 0.32−0.34 mmol of Ti/g of cat. Ethene and propene donated by Chisso Corp. were of research grade and were used without further purification. Triethylaluminum [TEA, $Al(C_2H_5)_3$, Tosoh Akzo Corp., Japan] was used as a toluene solution. Toluene was purified by passage through a 13X molecular sieve column.

Homopolymerization of Propene Using a High-Pressure-Type Stopped-Flow System. Olefin polymerization is typically performed in glass at a low monomer pressure or in stainless steel autoclaves at increased pressure. With this in mind, a high-pressure-type stopped-flow polymerization apparatus (two-vessel type, TEM-MH200, Taiatsu Techno Corp., Japan) was developed and is schematically illustrated in Figure 1. Features A and B are special pressure-resistant vessels equipped with water jackets. A toluene slurry (100 mL) of the catalyst and $Al(C_2H_5)_3$ solution in toluene (100 mL) were placed in vessels A and B, respectively. Propene was then introduced into the vessels through a mass-flow controller (STEC Inc., Japan, flow rate: 50 L/min) and then allowed to stand for 30 min at 30 °C. The monomer concentration of the aliphatic and aromatic hydrocarbons in the case of the ethene and propene polymerization is usually calculated using a monomer pressure−solubility correlation curve.[15] The propene concentration in toluene at 30 °C, which was estimated according to the correlation curve, was 1.69 mol/L at 4 atm and 3.19 mol/L at 6 atm. After the slurry and the solution attained equilibrium conditions, they were forced to simultaneously flow through the stainless steel tube from vessels A and B into a pressure preservation tank (C) with the pressure of propene. The polymerization of propene occurred in the stainless steel tube from X to Y, where the flow rate was adjusted by a pressure preservation valve (purge flow rate: 110 L/min) and digital pressure gauge (3.6 kgf/cm^2·G). The propene polymerizations at 4 and 6 atm were conducted with the catalyst (0.5 g, 0.16 mmol of Ti) and $Al(C_2H_5)_3$ (14 mmol, Al/Ti mole ratio = 88) in toluene at 30 °C for ca. 0.1 s.

Homopolymerization at atmospheric propene pressure (1 atm) was performed in a manner similar to the previously reported method.[7,9,16] The polymerization was conducted with the catalyst (1.4 g, 0.47 mmol of Ti) and $Al(C_2H_5)_3$ (14 mmol, Al/Ti mole ratio = 30) in toluene at 30 °C for ca. 0.1 s. The propene concentration (0.71 mol/L) in toluene at 30 °C was determined by gas chromatography (Yanaco G6800-CS-FS-G, Japan) with a porous polymer packed column (Waters Porapak Q, 50−80 mesh, 1.5 m, U.S.). After the polymerization was quenched at point Y with ethanol/HCl, the obtained polymer was washed three times with distilled water in order to remove the catalyst residues and then dried in vacuo at 60 °C for 2 h.

Synthesis of Block Copolymer Using a High-Pressure-Type Stopped-Flow System. A high-pressure-type apparatus comprised of three special vessels was used for the synthesis of the block copolymer and is schematically illustrated in Figure 2. The catalyst slurry (100 mL) and $Al(C_2H_5)_3$ solution (100 mL) of toluene were placed in vessels A and B, while toluene (100 mL) was placed in vessel C. The monomers were introduced into the vessels through the mass

flow controller (flow rate: 50 L/min) and then were allowed to stand for 30 min at 30 °C. The preparation of the block copolymers at 4 and 6 atm was conducted with the catalyst (0.5 g, 0.16 mmol of Ti) and $Al(C_2H_5)_3$ (14 mmol, Al/Ti mole ratio = 88) in toluene at 30 °C for 0.2 s. The propene and ethene concentrations in each vessel were 1.69 and 0.48 mol/L at 4 atm and 3.19 and 0.72 mol/L at 6 atm, respectively. The values were also estimated based on the monomer pressure−solubility correlation curves.[15] The polymerization of propene occurred in the stainless steel tube from point X to Y, and then the subsequent copolymerization of propene with ethene took place in the part from point Y to Z. The monomer conversions were held below 10% in order to neglect the changes of monomer concentrations and polymerization temperature. The polymerization time of each part was adjusted to 0.10 s to avoid any unfavorable chain-transfer reactions. A needle valve was used in the line from vessel C to point Y in order to keep a constant flow rate. A pressure preservation valve (purge flow rate: 110 L/min) and digital pressure gauge (3.6 kgf/cm^2·G) were also employed to control the flow rate. Shut off valves were required for the simultaneous start of the flow from each vessel. The polymerization was quenched at point Z; then, the obtained polymer was washed three times with distilled water and dried in vacuo at 60 °C for 2 h. The catalyst residues in the resulting block copolymers were removed by this treatment.

The preparation of the block copolymer at atmospheric pressure (1 atm) was carried out according to a previously reported method.[6,7,9,16] The propene and ethene concentrations in each vessel were 0.71 and 0.15 mol/L, respectively, which were determined by gas chromatography.

Characterization of Resulting Polymers. The molecular weight and molecular weight distribution of the polymers obtained in this study were determined using gel permeation chromatography (GPC, Senshu SSC-7100, Japan) with polystyrene gel columns (Tosoh TSK-GEL G3000HHR and TSK-GEL G5000HHR, Japan) at 140 °C using *o*-dichlorobenzene containing 2,6-di-*tert*-butyl-*p*-cresol (0.03 wt %) as an antioxidant. The molecular weight was calculated by the standard procedure based on the universal calibration curve of PP.

^{13}C NMR spectra were recorded with a Varian Gemini-300 spectrometer operated at 75 MHz with proton decoupling at 120 °C in 1,2,4-trichlorobenzene with 2,6-di-*tert*-butyl-*p*-cresol (0.03 wt %). Benzene-d_6 (25% v/v) was added as an internal lock, and a small amount of hexamethyldisiloxane was used for the internal chemical shift reference (2.03 ppm). The resulting polymers were analyzed according to a previously reported method.[17−20]

Melting temperature (T_m) and enthalpy of fusion (ΔH_f) of the polymer samples were measured by differential scanning calorimetry (Mettler-Toledo calorimeter DSC 820, U.S.) with the following conditions: heated from 50 to 230 °C at a heating rate of 10 °C·min^{-1}, held for 10 min, cooled to −100 °C at a cooling rate of 1.0 °C·min^{-1}, held for 10 min, heated from −100 to 230 °C at a scanning rate of 10 °C·min^{-1} (measurement of T_m) under a nitrogen atmosphere. The degree of crystallinity of PP (χ_c) was determined by following equation,[21,22]

$$\chi_c = \frac{\Delta H_f}{\Delta H_f^0} \tag{1}$$

where ΔH_f is the enthalpy of fusion obtained for a given PP, as measured by DSC. ΔH_f^0 (209 J/g) denotes the folded-chain PP crystal.[13,23] On the other hand, the enthalpy of fusion of the PP part in the PP-*b*-(PE-*co*-PP) ($\Delta H_{f,PP}$) is described by the following equation,

$$\Delta H_{f,PP} = \frac{Y_h}{Y_b} \cdot \Delta H_{f,block} \tag{2}$$

where Y_h and Y_b are the yields of the PP homopolymer corresponding to the PP part in the block copolymer and the PP-*b*-(PE-*co*-PP), respectively. $\Delta H_{f,\ block}$ is the enthalpy of fusion obtained for a given overall PP-*b*-(PE-*co*-PP). The degree of crystallinity of the block copolymer was also calculated using eq 1.

The crystallizability and its distribution of polymer samples obtained in this study were determined by cross-fractionation chromatography (CFC T-150A, Mitsubishi Petrochemical Co., Japan) with *o*-dichlorobenzene as an extraction solvent. Approximately 2 mg of sample (0.3 wt % *o*-dichlorobenzene) was loaded onto a glass bead packed column (4.6 mm diam, 150 mm) at 140 °C. The column was cooled to 0 °C at a slow cooling rate (8.4 °C/h), followed by stepwise elution from the column at 0, 10, 20, 30, 40, 50, 60, 64, 68, 72, 76, 80, 84, 88, 92, 96, 100, 103, 106, 109, 112, 115, 120, and 140 °C at a flow rate of 1.0 mL·min^{-1}. Each eluted polymer solution was automatically sent to the GPC section (Shodex AD-806NS, Showa Denko K. K., Japan) of the CFC system equipped with an infrared detector.

Supermolecular structures of the PP homopolymers and PP-*b*-(PE-*co*-PP)s obtained at 1 and 6 atm were observed with the polarizing microscopy (Olympus BX50-33PO/U-POC, Japan) and atomic force microscopy (AFM). AFM images were recorded with a Nanoscope III multimode AFM (Digital Instruments, Santa Barbara, U.S.), operated in air in both the contact and tapping modes using microfabricated cantilevers with spring constant in the range 0.06−0.6 N/m for the contact mode and 30 N/m in the case of tapping mode. The preparation procedure of solution-cast films suitable for microscopic observations was as follows. Aliquots (1−2 drops) of the polymer sample dissolved in *o*-dichlorobenzene at a concentration of 0.5 wt % were deposited on the surface of glass slide, which was located on the hot stage at a fixed temperature. To achieve the spherulites with greater size under optimal conditions, the treating temperature was chosen in the range 130−140 °C. Evaporation time was on the order of 1−2 min, and the crystallization time was in the range 0.25−7 h. Irganox 1010 and Irgafos 168 as an antioxidants were used with the concentration in the dry polymer sample of 0.1 wt %.

Results and Discussion

In the industrial process, the production of polypropylene is generally performed for 1−3 h depending upon the type of process. In contrast, the polymerization can be conducted within an extremely short period (ca. 0.1 s) using the stopped-flow technique.[16] For olefin polymerization with a typical Ziegler catalyst, catalyst deactivation, as well as the various types of chain-transfer reactions, proceeds with the propagation reaction. On the other hand, the states of the active sites are constant without a time-dependent change, and chain-transfer reactions can be considered negligible within the extremely short period. It should be noted that the appropriate choices of suitable polymerization conditions and catalyst systems are required in order to fully utilize the ability of the stopped-flow technique for the synthesis of the block copolymer having a controlled molecular weight. Prior to the synthesis of the block copolymer, therefore, the effect of monomer pressure on the stopped-flow polymerization of propene was investigated using the high-pressure-type stopped-flow system developed by our research group.

Homopolymerization of Propene Using a High-Pressure-Type Stopped-Flow System. The influence of the monomer pressure in the system, namely, the monomer concentration, on the yield, molecular weight, molecular weight distribution, and microtacticity of PP was investigated as a preliminary study. A number of studies have proven the dependence of the polymerization rate on the propene concentration over a broad range of the concentration using $TiCl_3$ and $MgCl_2$-supported catalysts.[24−28] A deviation from the first-order dependence was, in some cases, found only at low

Table 1. Propene Polymerization with an $MgCl_2$-Supported Catalyst and TEA at 30 °C for 0.1 s in Toluene under Different Monomer Pressures

code	propene pressure (atm)	$[M_{C_3H_6}]$ (mol/L)	yield (g/mol of Ti)	$\bar{M}_n$[a]	$\bar{M}_w/\bar{M}_n$[a]	*mmmm*[b] (%)
P-1[c]	1	0.71[d]	500	9 500	3.2	87.8
P-2[e]	4	1.69[f]	1100	24 000	2.8	86.5
P-3[e]	6	3.19[f]	2300	43 000	3.1	86.3

[a] Molecular weight and its distribution were determined by GPC. [b] Meso pentad fraction (*mmmm*) was determined by ^{13}C NMR. The polymerization was conducted with [c]atmospheric-pressure- and [e]high-pressure-type stopped-flow methods. Propene concentration was determined by gas chromatography,[d] and was calculated according to the monomer pressure−solubility correlation curve (Kruis and Hausen[15]).[f]

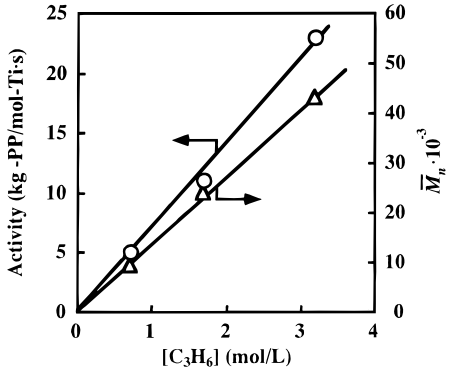

Figure 3. Dependence of propene concentration on catalyst activity (○) and the number-average molecular weight of PP (△).

monomer concentrations. Recently, several interesting reports have been published with regard to the correlation of the monomer pressure with the isotacticity of PP obtained with various catalysts.[29−35] Busico et al. have reported that the monomer concentration significantly affected the isotacticity of PP obtained with the $MgCl_2/TiCl_4-Al(C_2H_5)_3$ catalyst system at low monomer pressures (less than 0.5 mol/L),[34] whereas the meso pentad fraction of PP obtained with the internal donor-free $MgCl_2/TiCl_4-Al(i\text{-}C_4H_9)_3$ catalyst system was almost unchanged in the monomer concentration regions of 0.1 to 0.47 mol/L (propene pressures between 0.35 and 1.0 atm) as reported by Soga et al.[35] On the basis of these facts, the monomer pressure was adjusted in this study to be greater than atmospheric pressure (1 atm).

The propene polymerization was carried out in toluene at 30 °C for ca. 0.1 s using the high-pressure-type stopped-flow apparatus at 1, 4, and 6 atm, and the results of this are summarized in Table 1. The increase in propene pressure induces increases in the polymer yield and molecular weight of PP, which are linearly proportional to the propene concentration, as can be seen in Figure 3. During polymerization without a chain-transfer agent, in principle, the molecular weight is dependent on the monomer concentration if chain transfer with monomer is important. Therefore, the linear relationship between the molecular weight and the propene concentration indicates that chain transfer with propene is clearly unimportant under the conditions used in this study or is compensated by the increase in the propagation rate. It is clear that the polymerization rate is first-order in propene concentration. Figure 4 shows the GPC curves of the PPs obtained at 1, 4, and 6 atm. The GPC curve clearly

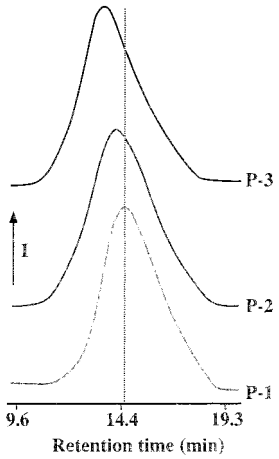

Figure 4. GPC curves of PPs obtained at 1 (P-1), 4 (P-2), and 6 atm (P-3).

shifted toward higher molecular weights with increasing propene pressure. All PP homopolymers show unimodal curves with similar molecular weight distributions ($\bar{M}_w/\bar{M}_n$ = 2.8−3.2), independent of the propene pressure. The values of microtacticity of the resulting PPs also remained unchanged (*mmmm* = ca. 87%). Hence, it was determined that the monomer pressure affected only the polymer yield and molecular weight but had no significant influence on the molecular weight distribution and microtacticity. There are essentially four modes of chain transfer in propene polymerization, that is, transfer via cocatalyst interactions, β-hydrogen transfer, monomer-assisted transfer, and hydrogenation when hydrogen is used as a chain-transfer agent. The result of the stopped-flow polymerization conducted as a function of the time at 1 atm was reported in our previous paper.[7] It was demonstrated that the polymer yield and the number-average molecular weight of the PP were proportional to the polymerization time up to about 0.2 s, at which the values of the molecular weight distribution were almost constant. Additionally, there was no induction period. These results indicated that the states of the active sites are constant without time-dependent change and that the aforementioned four chain-transfer reactions can be effectively negligible under these conditions. In this study using the high-pressure stopped-flow system, a linear correlation of the monomer pressure with the molecular weight was found, suggesting that the chain-transfer reaction with the monomer can be negligible even at higher monomer pressures. The possibility of the other three chain-transfer reactions is also considered to be very low in the stopped-flow propene polymerization. On the basis of results from the linear relation of the polymerization time to the catalyst activity reported in our previous study[7] and the linear relation of the monomer pressure to the catalyst activity obtained in this study, it has been substantiated that prolonged polymerization time and increased monomer pressure have no significant influence on the states of the active sites on the catalyst under the conditions used in this study. Hence, it was verified that the high-pressure-type stopped-flow polymerization technique was applicable for the production of an olefin block copolymer having a controlled molecular weight.

Synthesis of Polypropene-*block*-poly(ethene-*co*-propene) Using a High-Pressure-Type Stopped-Flow System. The synthesis of the block copolymer was

Table 2. Synthesis of PP-*b*-(PE-*co*-PP) with an $MgCl_2$-Supported Catalyst and TEA at 30 °C in Toluene under Different Monomer Pressures[a]

code	monomer concentration (mol/L) vessel A $[M_{C_3H_6}]$	vessel B $[M_{C_3H_6}]$	vessel C $[M_{C_2H_4}]$	$[M_{C_2H_4}]/[M_{C_3H_6}]$	yield (g/mol of Ti)	$\bar{M}_n$[b]	$\bar{M}_w/\bar{M}_n$[b]	ethene content[c] (mol %)
B-1[d]	0.71	0.71	0.15	0.11	1300	14 000	3.0	27.3
B-2[e]	1.69	1.69	0.48	0.14	3200	33 000	2.8	28.1
B-3[e]	3.19	3.19	0.72	0.09	6000	60 000	2.8	23.7

[a] Polym. time in seconds (PP:PE-*co*-PP) = 0.10:0.10. [b] Molecular weight and its distribution were determined by GPC. [c] Ethene content in PP-*b*-(PE-*co*-PP) was determined by ^{13}C NMR. The polymerization was conducted with [d]atmospheric pressure- and [e]high-pressure-type stopped-flow methods.

Table 3. Block Composition and Ethene Content in PE-*co*-PP Part in the Block Copolymer[a]

code	block composition (wt %)[b] PP	PE-*co*-PP	ethene content in[c] PE-*co*-PP part (wt %)
B-1[d]	38.5	61.5	32.5
B-2[e]	34.4	65.6	31.6
B-3[e]	38.3	61.7	27.9

[a] Polymerization time in seconds (PP:PE-*co*-PP) = 0.10:0.10. [b] Block composition was calculated from the results of polymer yields of PP and PP-*b*-(PE-*co*-PP); see Tables 1 and 2. [c] Ethene content in PE-*co*-PP part in the block copolymer was calculated from the results of block composition and the overall ethene content in the block copolymer obtained from ^{13}C NMR. The polymerization was conducted with [d]atmospheric pressure- and [e]high-pressure-type stopped-flow methods.

carried out at different ethene and propene pressures (1, 4, and 6 atm) with the $MgCl_2$-supported Ziegler catalyst and TEA at 30 °C using the high pressure-type stopped-flow apparatus, as shown in Figure 2. The polymerization time of each part was adjusted to be ca. 0.1 s. These results are summarized in Table 2. The molecular weight of the resulting block copolymer was found to increase with increasing monomer concentrations. The molecular weight of the block copolymer (B-3, $\bar{M}_n$ = 60 000) obtained at 6 atm is considered to be higher than the critical molecular weight of the block copolymer, which is typically several times higher than the molecular weight per entangled unit (the value of PP has been reported to be 4650[36] or 2900[37]), depending upon the structure of the polymer. The achievement of the block copolymer having a molecular weight higher than that of this value is very essential to fulfilling the properties of a polymer having a well-defined crystalline-amorphous microstructure and desirable performance. The molecular weight distributions of the block copolymers were almost the same regardless of the difference in monomers pressures. This behavior is similar to the case of propene homopolymerization using the high-pressure-type stopped-flow method described in the previous section. Table 3 shows the block composition of the PP-*b*-(PE-*co*-PP) calculated from the results of the yields of PP (see Table 1) and PP-*b*-(PE-*co*-PP) (see Table 2) as well as the ethene content in the PE-*co*-PP part in the block copolymer calculated from the results of the block composition and the overall ethene content in the block copolymer obtained by ^{13}C NMR. The ethene content and block composition in the block copolymer were not constant, which may be due to the deviation of the solubility of ethene and propene for each actual monomer pressure in the monomer pressures−solubility correlation curve in toluene. The ethene and propene concentrations in toluene have been found to drastically increase with pressure, but the tendency of ethene is different from that of propene. Therefore, the total $[C_2H_4]/[C_3H_6]$ ratio was different for each case, as can be seen in Table 2, which contributes

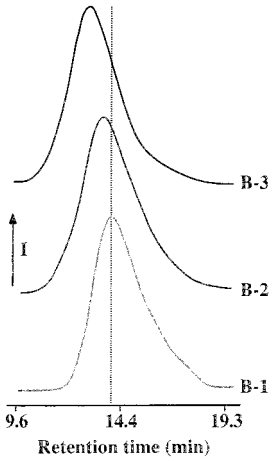

Figure 5. GPC curves of block copolymers obtained at 1 (B-1), 4 (B-2), and 6 atm (B-3).

to the variations in the ethene content and the block composition of the PE-*co*-PP segment in the block copolymer. Figure 5 shows the GPC curves of the block copolymers obtained at 1, 4, and 6 atm. The block copolymers show unimodal GPC curves with similar molecular weight distribution values ($\bar{M}_w/\bar{M}_n$ = 2.8−3.0). The increases in the monomer pressures were found to induce the GPC curve to shift toward the higher molecular weight region without any peak in the low-molecular-weight region. Thus, it was clear that the polymer yield and the molecular weight of the block copolymer increased with monomer pressures, while the time-dependent change in the molecular weight distribution was negligibly small. On the basis of these results, combined with that of the propene homopolymerization, it may be reasonable to consider that the chain-transfer reaction with the monomer can be negligible and that the states of the active sites on the catalyst are little affected by the monomer pressures under the conditions used for the synthesis of the block copolymers. The constant value of the molecular weight distribution of the block copolymers obtained at different monomer pressures indicates that there is no change in the relative amounts of the different types of the active sites existing on the catalyst. These results also indicate that the molecular weight, the composition of the block segments, and the microstructure of the PE-*co*-PP segment in the block copolymer can be adjusted by controlling the monomer pressures.

To obtain further information on the influence of monomer pressure on the composition and microstructure, the block copolymers obtained at 1, 4 and 6 atm were extracted with heptane, and the microstructures of the extracted copolymers were analyzed by ^{13}C NMR spectroscopy. It may safely be assumed that the modified stopped-flow technique can lead to three types of

Table 4. Results of Triad Sequence Distribution and Ethene Content of PP-*b*-(PE-*co*-PP)s

sample[a]	extraction[b]	amount of insoluble part (wt %)	triad sequence distribution (mol %)[c]						ethene content[c] (mol %)	SD[d]
			PPP	PPE	EPE	PEP	PEE	EEE		
B-1	before		53.9	14.0	4.8	7.7	10.1	9.5	27.3	
	after	76.2	66.1	9.5	3.6	5.9	4.6	10.3	20.8	5.8
B-2	before		54.8	12.5	4.6	7.8	7.2	13.1	28.1	
	after	86.0	58.1	13.1	5.1	7.3	6.9	9.5	23.8	2.0
B-3	before		55.2	15.7	5.5	6.8	7.2	9.6	23.7	
	after	96.3	58.1	13.8	4.3	7.0	7.2	9.6	23.8	1.5

[a] See Table 2. [b] Extraction experiment was performed by soxhlet-type extractor with *n*-heptane at room temperature for 24 h. [c] Triad sequence distribution and ethene content were determined by ^{13}C NMR. [d] Standard deviation was calculated using the equation of $\sigma = \sqrt{1/n \cdot \sum_{i=1}^{n}(x_i - \bar{x})^2}$ ($n = 6$), where x_i and $\bar{x}$ are triad frequencies in the block copolymer before and after extraction, respectively.

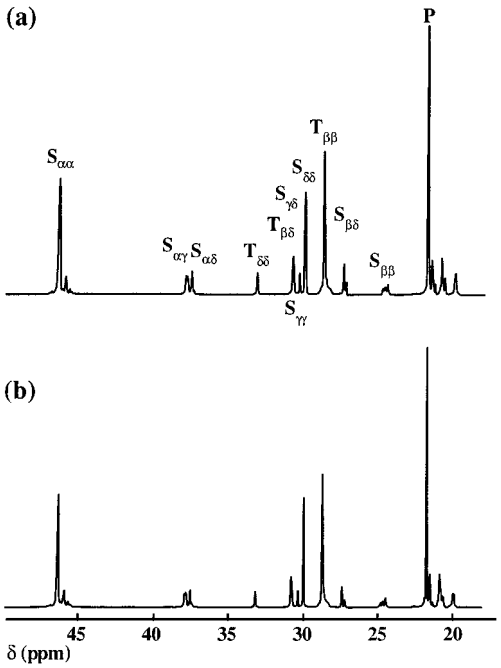

Figure 6. ^{13}C NMR spectra of the block copolymer obtained at 6 atm (a) and the unsolved part of the block copolymer after extraction with heptane (b).

polymers: PP homopolymer (formed by chain termination prior to ethene addition), PE-*co*-PP (formed by chain initiation following ethene addition), and the desired PP-*b*-(PE-*co*-PP). It is practically difficult to detect the possibility of the existence of the PP homopolymer in the final product at the present time. However, the ^{13}C NMR analysis of the fractionated block copolymers may suggest that the formation of PP homopolymer by chain termination prior to ethene addition can scarcely occur under these conditions.[38] The amount of the PE-*co*-PP can be determined by measuring the amount of the soluble fraction after extraction. The extraction was carried out at room temperature for 24 h in a manner similar to the previously reported method.[6,7,39] Figure 6 shows the ^{13}C NMR spectra of the block copolymer obtained at 6 atm and its extraction residues. Tertiary and secondary carbon atoms are denoted as T and S, respectively, with two Greek subscripts indicating the position relative to the nearest tertiary carbon atoms in both directions along the polymer chain. Signals at δ = 37.9−38.4, 37.5, 33.2, 30.9−31.2, 30.4, 30.0, 27.4, and 24.7 ppm, from $S_{\alpha\gamma}$ in 2PEP, $S_{\alpha\delta}$ in PEE, $T_{\delta\delta}$ in EPE, $T_{\beta\delta}$ in PPE, $S_{\gamma\delta}$ in PEEE, $S_{\delta\delta}$ in EEE, $S_{\beta\delta}$ in PEE, and $S_{\beta\beta}$ in PEP, respectively, were attributed to PE-*co*-PP, and signals at 45.7−46.6, 29.0, and 21.8−20.0 ppm, from $S_{\alpha\alpha}$ in PP, $T_{\beta\beta}$ in PPP, and P, respectively, were mainly due to the PP homopolymer.[19,20] The values of the amount of the insoluble part, the triad sequence distribution, the ethene content, and the standard deviation (SD) of the block copolymers before and after the extraction are summarized in Table 4. The amount of the insoluble part in the resulting block copolymer was found to increase with the monomer pressures, and only a small amount (3.7 wt %) was soluble in the block copolymer obtained at 6 atm. This phenomenon is considered to be governed by the fact that the increased monomer pressures induced the decrease in PP-*b*-(PE-*co*-PP) having a PP part with a shorter chain length, which is soluble even in heptane at room temperature. In our previous study, it was clear that the signals from PE-*co*-PP disappeared completely after the extraction in the cases of the commercial block-type copolymer and PP/PE-*co*-PP blend, which have no chemical linkage between the two segments.[6,7] In the case of the block copolymers obtained in this study at lower monomer pressures, the slight decreases in the peak intensities arising from PE-*co*-PP may be due to the lower molecular weight. For the block copolymer obtained at 6 atm, however, no significant difference in the intensities of these peaks was observed before and after the extraction. Furthermore, the standard deviation was very small. These results clearly indicate the formation of PP-*b*-(PE-*co*-PP), where the PE-*co*-PP is chemically linked to the PP, having a variable molecular weight.

Characterization of Resulting Block Copolymers. From the aspect of crystallization in polyolefins, the influence of molecular weight is very important. Hence, an understanding of the correlation of the molecular weight to the crystallization and crystalline morphology of the block copolymer was considered to be required for developing a novel polyolefin with outstanding performance. Along with the practical importance, we investigated the crystalline morphology and supermolecular structure of the block copolymers having a different molecular weight using differential scanning calorimetry (DSC), cross-fractionation chromatography (CFC), polarizing microscopy, and AFM.

The crystallizability of a polymer chain is a critical factor which depends on the crystallinity and lamellar thickness. As is well-known, the melting temperature (T_m) is related to the lamellar thickness, and the enthalpy of fusion (ΔH_f) depends on the degree of crystallinity. Thus, the resulting block copolymers and PP homopolymers obtained at 1 and 6 atm were analyzed by DSC, the results of which are presented in Table 5. In both cases, the PP-*b*-(PE-*co*-PP)s exhibit a lower melting temperature compared with that of PP homopolymers. It is suggested that the depressing of the recrystallization or the rearrangement process of the

Table 5. Thermal properties and degree of crystallinity of PPs and PP-*b*-(PE-*co*-PP)s

		ΔH_f (J/g)		
sample[a]	T_m[b] (°C)	obsd[b]	calcd[c]	χ_c[d] (wt %)
P-1	158	123		59
B-1	154	33	86	41
P-3	160	119		57
B-3	159	34	89	42

[a] See Tables 1 and 2. [b] Melting temperature (T_m) and heat of fusion (ΔH_f) of polymers were observed by DSC. [c] Heat of fusion of PP part in the PP-*b*-(PE-*co*-PP)s was calculated from eq 2; see Experimental Section. [d] Degree of crystallinity (χ_c) was calculated from eq 1; see Experimental Section.

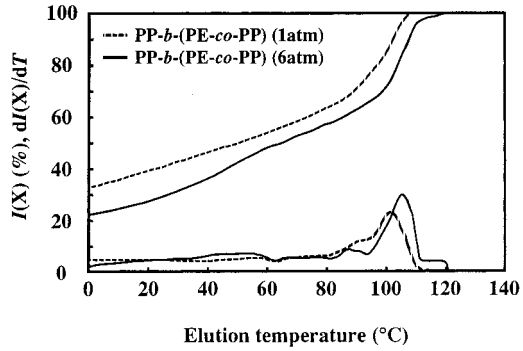

Figure 7. Temperature rising elution fractionation diagrams of PP-*b*-(PE-*co*-PP)s obtained at 1 (B-1) and 6 atm (B-3).

PP crystal is due to the chemically linked PE-*co*-PP part to produce a thinner crystal.[8] The melting temperature of the block polymer obtained at 6 atm was apparently higher than that obtained at 1 atm, indicating that the higher molecular weight of the block copolymer may lead to a greater lamellar thickness. The PP homopolymers obtained at 1 and 6 atm also showed the same tendency, while the difference in ΔH_f between the block polymers prepared at different monomers pressures was observed to be very small. There were also no significant differences between the degrees of crystallinities for the PP part in the block copolymers. This means that the increased molecular weight of the block copolymer had no effect on the degree of crystallinity but had an influence only on the lamellar thickness during the melt−crystallized process in this study.

The CFC technique[40] is considered to be suitable for the evaluation of the crystallinity, crystallinity distribution, and crystallizability of the block copolymer. A comparison of the structural heterogeneity between the block copolymers obtained at 1 and 6 atm was made by means of CFC. Temperature rising elution fractionation diagrams (differential type) of the PP-*b*-(PE-*co*-PP)s are shown in Figure 7. There were two different peaks in the region of 80−120 °C. The observed multiple peaks are thought to be mainly due to the difference in the isotacticity of the PP part in the resulting block copolymer, on the basis of the result that a bimodal distribution was also observed in the PP homopolymer prepared by the stopped-flow polymerization.[7] It is considered that the lower elution temperature of the block copolymer compared with the PP homopolymer is governed by the effect of the chemically linked PE-*co*-PP part on the crystallization of the PP part in the block copolymer. The main peak at 105 °C was observed in the case of PP-*b*-(PE-*co*-PP) obtained at 6 atm, which was apparently higher than that obtained at 1 atm. These results suggest that the higher molecular weight of the block copolymer may lead to a greater crystallizability of PP

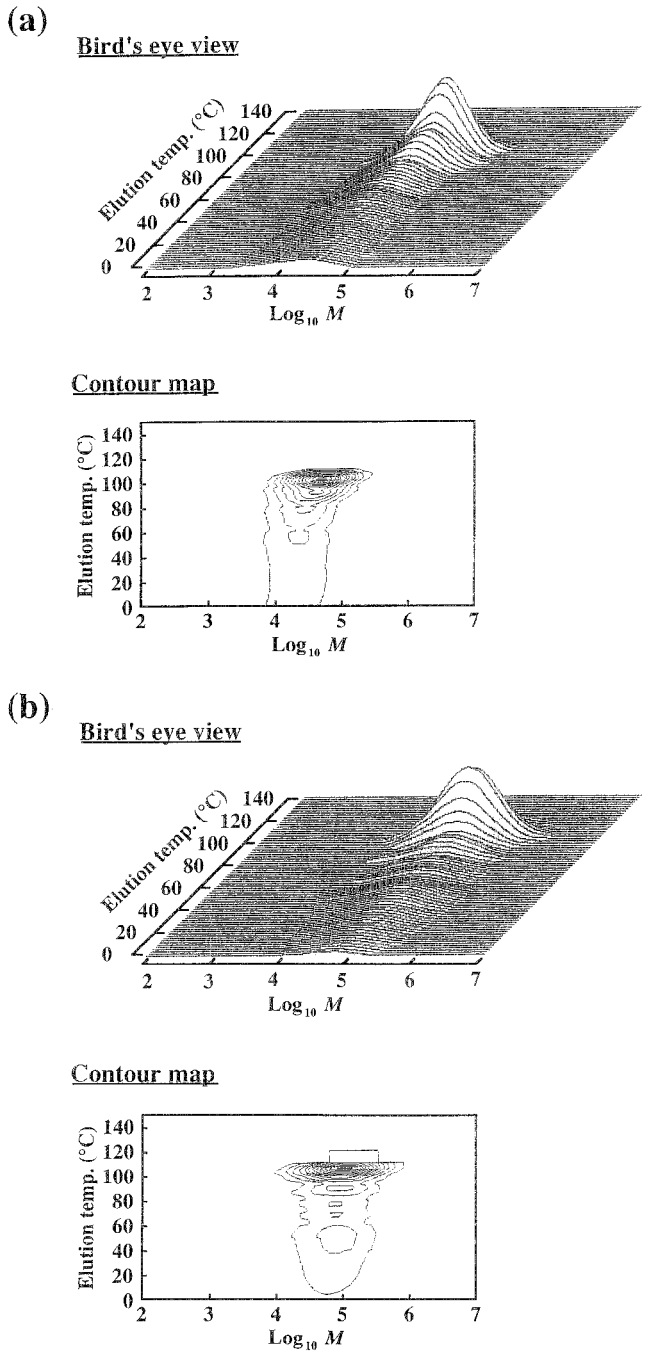

Figure 8. Bird's eye views and contour maps of PP-*b*-(PE-*co*-PP)s obtained at (a) 1 (B-1) and (b) 6 atm (B-3).

part. In other words, the depression of the recrystallization or rearrangement process of the PP crystal, which is due to the chemically linked PE-*co*-PP part, was reduced by the increased molecular weight, resulting in a increase of lamellar thickness.

Figure 8 shows the bird's eye views (differential-type) of PP-*b*-(PE-*co*-PP)s as well as the corresponding contour maps. This figure clearly shows that PP-*b*-(PE-*co*-PP)s eluted at each temperature region between 0 and 120 °C are mainly composed of a uniform component, regardless of the difference in monomer pressures. The appearances of bird's eye views and contour maps of the resulting PP-*b*-(PE-*co*-PP)s remained without change, suggesting the increased molecular weight of the block copolymer had no effect on the crystallinity and crystallinity distribution. It is also clear that the GPC peaks

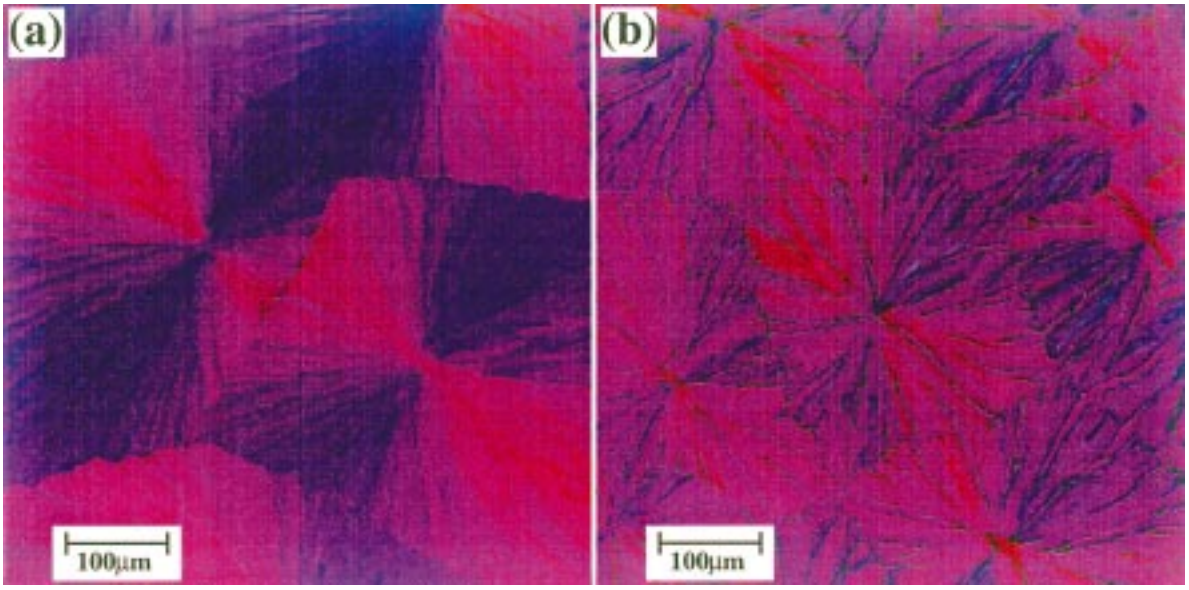

Figure 9. Polarizing micrographs of the spherulites of PP-*b*-(PE-*co*-PP)s obtained at (a) 1 (B-1) and (b) 6 atm (B-3). The samples were prepared at 140 °C for 7 h. The color of the spherulites in both micrographs corresponds to positive birefringence.

Table 6. Characterization of Fractionated Block Copolymers Obtained at 1 and 6 atm

	1 atm[a]			**6** atm[b]		
elution temp. (°C)	wt fraction[c] (%)	$\bar{M}_n$[d]	$\bar{M}_w/\bar{M}_n$[d]	wt fraction[c] (%)	$\bar{M}_n$[d]	$\bar{M}_w/\bar{M}_n$[d]
0−30	42.1	10 000	2.4	31.1	23 000	2.8
30−45	5.4	14 000	2.1	7.7	42 000	2.6
45−82	16.8	17 000	1.8	18.9	47 000	2.5
82−96	13.7	27 000	1.8	9.4	59 000	2.1
96−112	22.0	38 000	1.8	30.2	66 000	2.4
112−120	n.d.[e]	n.d.[e]	n.d.[e]	2.7	110 000	2.2

[a] Sample B-1 and [b]sample B-3; see Table 2. [c] Weight fraction eluted at each temperature was estimated from the data of TREF section of CFC system. [d] Molecular weight and its distribution were determined by the GPC section of the CFC system. [e] n.d.: not detected.

of each fraction of the PP-*b*-(PE-*co*-PP) eluted at different temperatures shift toward higher molecular weight region by increasing monomer pressures from 1 to 6 atm. Hence, the formation of the block copolymer having a higher molecular weight was confirmed by the substantial shift of the GPC profiles of each fraction to higher molecular weight.

On the basis of the results, the fractionation of the block copolymers was conducted to divide into six fractions, the results of which are shown in Table 6. Each fraction was found to possess a narrow molecular weight distribution ($\bar{M}_w/\bar{M}_n \approx 2$) with a different molecular weight.[41] In all fractions, the molecular weights of the PP-*b*-(PE-*co*-PP) obtained at 6 atm were higher than those obtained at 1 atm. Further, the weight fraction eluted at 30−120 °C was observed to increase with increasing monomer pressures. On the basis of these results, it was substantiated that the increased molecular weight induced a greater crystallizability but had no influence on the crystallinity and crystallinity distribution of the block copolymer.

Microscopy, e.g., polarizing microscopy, scanning electron microscopy, and transmission electron microscopy, is a major technique for the assessment of the structure of the semicrystalline polymers.[42] The supermolecular structure including spherulites and axialites

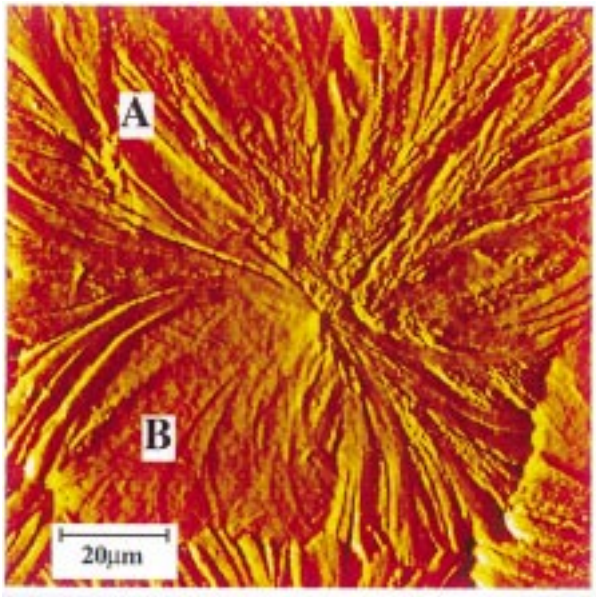

Figure 10. Large-scale contact mode (deflection) AFM image of the spherulite of PP-*b*-(PE-*co*-PP) obtained at 6 atm (B-3) having sheaflike morphology. The sample was prepared at 130 °C for 20 min. (A) Sheaflike region. (B) Region surrounding the sheaf.

is conveniently observed by polarizing microscopy. Here, the polarizing microscopy was applied to confirm the structural difference between the block copolymers obtained at 1 and 6 atm. Polarizing microscopic observation showed that at elevated temperatures both block copolymers may produce spherulites with a size of up to several hundred micrometers (Figure 9) and that their morphology follows general tendencies found for PP spherulites.[43,44] However the spherulites always had positive birefringence and revealed higher tendencies to form the sheaflike structures.[44] The positive birefringence of both samples indicate that crosshatching, which vanishes for the usual isotactic PP at elevated temperatures, still remained for the block copolymers even at the temperature of 150 °C. There were slight difference in the spherulite size and its structure between two block copolymers. Notice also that in both cases the

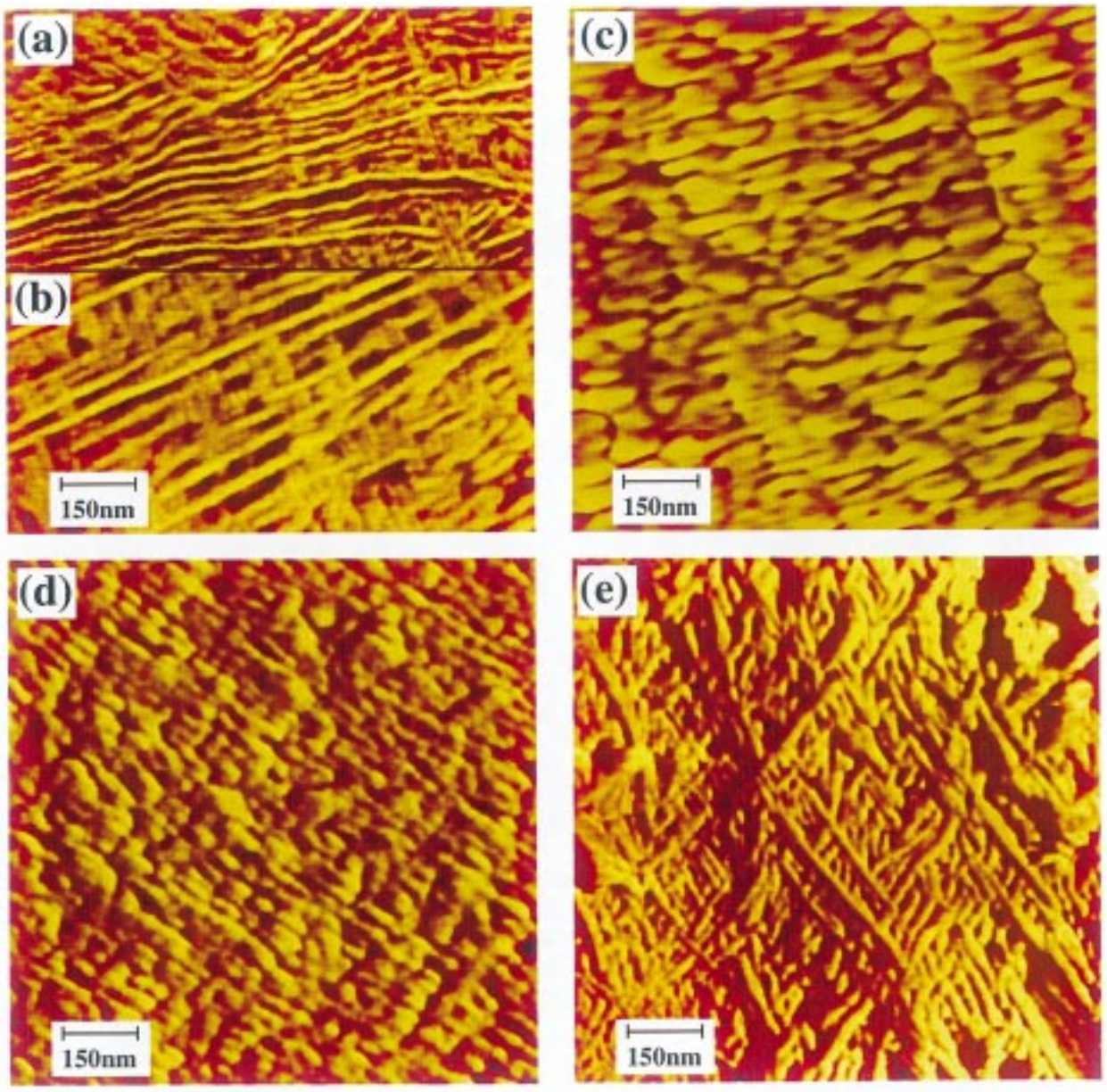

Figure 11. AFM images of lamellar structures for the spherulites of the block copolymers and PP homopolymers. Images a−d were received in tapping mode (phase), and image e was received in contact mode (friction). The images correspond to PP-*b*-(PE-*co*-PP) obtained at 6 atm (B-3, crystallization conditions: 130 °C, 20 min) located in the sheaflike region (a) and in the region surrounding the sheaf (b), which correspond to Figure 10; (c) PP homopolymer obtained at 6 atm (P-3, crystallization conditions: 130 °C, 15 min); (d) PP-*b*-(PE-*co*-PP) obtained at 1 atm (B-1, crystallization conditions: 140 °C, 35 min); and (e) PP homopolymer obtained at 1 atm (P-1, crystallization conditions: 140 °C, 30 min).

spherulites often had wide gaps between their radial branches, as shown in Figure 9b.

AFM is a high-resolution method which sensitively records the surface topography and which has great potential for nonconductive materials such as polymers.[42] Scanning force microscopy provides information about local variations in the mechanical properties in a sample and may thus reveal local variations in chain orientation and composition. In this study, the crystalline morphology including the interlamellar distances of the PP homopolymers as well as PP-*b*-(PE-*co*-PP)s obtained was investigated by AFM. The latter was determined from higher resolution AFM images. Figure 10 shows the large-scale contact mode (deflection) AFM image of the spherulite of PP-*b*-(PE-*co*-PP) obtained at 6 atm. The sheaflike structure of the spherulite is observed in the AFM image. The measurements of the interlamellar distances were performed, resulting in a great dispersion for this parameter for all of the samples even within particular chosen spherulite. In particular, the lateral regions surrounding the sheaf (region B) showed systematically more thickened lamellae with the distances between them in the range 30−50 nm in comparison with regions inside the sheaf (region A). The same high values were observed for quadrite-type structures for the samples prepared at the same conditions in our previous paper.[8] Notice that both these above-mentioned morphological types have a high degree of crosshatching and have no usual radial features inherent to spherulites. The interlamellar distances inside the spherulites, if not taking into consideration those regions with much higher values, had lower values in the range 15−30 nm. This broad size distribution is probably due to the chosen isothermal mode of crystal-

lization resulting to crystallite thickening.[45] Minimal observed interlamellar distances were in the range 14−17 nm for all substances.

Figure 11a,b represents the phase images of two regions of the same spherulite of the PP-*b*-(PE-*co*-PP) obtained at 6 atm (sample prepared at 130 °C for 20 min) with interlamellar distances lying correspondingly in the range 16−25 nm for part a and 25−30 nm for part b. Too-wide dispersion does not allow for a comparison of the mean interlamellar distances for the block copolymers and PP homopolymer, but the received results indicate that the differences, if they exist, are relatively small.

On the basis of the result mentioned above, the AFM observations of the block copolymers and PP homopolymers were conducted in the sheaf region. If sheaflike structures were analyzed, the two or more times difference in long period was expected on the grounds of the hypothesis that the crystalline layer thickness is the same for the block copolymer and PP homopolymer. However, the interlamellar distance values on these samples were approximately the same in the sheaf region, as can be seen in Figure 11. This is an indication that the block copolymers and PP homopolymers have the same long period, regardless of the molecular weight. Here, it must be noted that the block copolymer obtained by the stopped-flow polymerization technique is not pure PP-*b*-(PE-*co*-PP) and that it contains a certain amount of PP homopolymer and amorphous PE-*co*-PP. On the basis of the results obtained in this study, however, it is considered that there are no significant differences in the relative amounts of the component (desired PP-*b*-(PE-*co*-PP), PP, and PE-*co*-PP) regardless of the monomer pressures, which affects only the molecular weight of the resulting polymers. Therefore, these results also suggest that the increased molecular weight of the block copolymer as well as PP homopolymer obtained at higher monomer pressure had no effect on the ratio of the amorphous layer thickness and the lamellar crystal thickness, which corresponds to the degree of crystallinity.

Conclusions

In this article, a high-pressure-type stopped-flow polymerization system has been introduced as a useful technique for the design and synthesis of novel polyolefins having a controlled crystalline−amorphous microstructure and desirable properties. The results of the homopolymerization of propene indicated that the change in propene concentration only induced a variation in the polymer yield and molecular weight but did not exert any influence on the molecular weight distribution and isotacticity of PP. No influence of the monomer pressure on the characteristics of the stopped-flow polymerization in which the catalyst activity is constant and the unfavorable side reactions can be negligible was confirmed by this study. The higher propene and ethene concentrations, which could be regulated by the monomer pressures, were found to induce a higher molecular weight of the resulting block copolymer without a significant change in the molecular weight distribution and the microstructure. The block copolymer having a molecular weight higher than that of the entanglement molecular weight was achieved by using this method, which was very essential to fulfill the properties of a polymer having a well-defined crystalline−amorphous microstructure and desirable performance. The increased molecular weight of the block copolymer was found to lead to a greater lamellar thickness without any change in the crystallinity and its distribution, which was substantiated by the characterization of the resulting polymers. The high-pressure-type stopped-flow polymerization system enabled us to synthesize the block copolymer, PP-*b*-(PE-*co*-PP), in which molecular weight, composition of the block segments, microstructure of the PE-*co*-PP segment, and crystalline morphology of the block copolymer can be adjusted by controlling the monomer pressures. This finding will perhaps in the future lead to crystalline−amorphous olefin block copolymers having a well-defined structure.[46]

Acknowledgment. The authors thank the Chisso Corp., Toho Titanium Co., Ltd., and Tosoh Akzo Corp. for their support and donation to our laboratory.

References and Notes

(1) Keii, T. Isotacticity and Molecular Weight of Ziegler−Natta Polymers. In *Kinetics of Ziegler−Natta Polymerization*; Kodansha: Tokyo, 1972; pp 89−128.
(2) Boor, J. Termination of Polymer Chain. In *Ziegler−Natta Catalyst and Polymerizations*; Academic Press: New York, 1979; pp 244−260.
(3) Kissin, Y. V. Stereospecificity of Heterogeneous Ziegler−Natta Catalysts. In *Isospecific Polymerization of Olefins*; Springer-Verlag: New York, 1985; pp 221−321.
(4) Albizatti, E.; Giannini, U.; Collina, G.; Noristi, L.; Resconi, L. Catalyst and Polymerizations. In *Polypropylene Handbook*; Moore, E. P., Jr., Ed.; Hanser Publishers: Munich, Germany, 1996; pp 11−110.
(5) Barbe, P. C.; Cecchin, G.; Noristi, L. *Adv. Polym. Sci.* **1987**, *81*, 1.
(6) Mori, H.; Yamahiro, M.; Tashino, K.; Ohnishi, K.; Nitta, K.; Terano, M. *Macromol. Rapid Commun.* **1995**, *16*, 247.
(7) Yamahiro, M.; Mori, H.; Nitta, K.; Terano, M. *Macromol. Chem. Phys.* **1999**, *200*, 134.
(8) Nitta, K.; Kawada, T.; Prokhorov, V. V.; Yamahiro, M.; Mori, H.; Terano, M. *J. Appl. Polym. Sci.*, in press.
(9) Yamahiro, M.; Mori, H.; Nitta, K.; Terano, M. *Polymer*, **1999**, *40*, 5265.
(10) Nitta, K.; Kawada, T.; Yamahiro, M.; Mori, H.; Terano, M. *Rep. Prog. Polym. Phys. Jpn.* **1997**, *40*, 335.
(11) Nitta, K.; Kawada, T.; Yamahiro, M.; Mori, H.; Terano, M. *Polymer*, submitted for publication.
(12) Duca, D. D.; Moore, E. P., Jr. End-Use Properties. In *Polypropylene Handbook*; Moore, E. P., Jr., Ed.; Hanser Publishers: Munich, Germany, 1996; pp 237−254.
(13) Mark, J. E.; Eisenberg, A.; Graessley, W. W.; Mandelkern, L.; Samulski, E. T.; Koenig, J. L.; Wignall, G. D. The Crystalline State. In *Physical Properties of Polymers*, 2nd ed.; American Chemical Society: Washington, DC, 1993; pp 145−200.
(14) Fatou, J. G. Morphology and Crystallization in Polyolefins. In *Handbook of Polyolefins*; Seymour, R. B., Vasile, C., Eds.; Marcel Dekker: New York, 1993; pp 155−227.
(15) Kruis, A.; Hausen, H. Diagramme und Tabellen. geordnet nach Lösungsmitteln. In *Landolt-Börnstein, IV. Band, Technik*; Borchers, H., Hausen, H., Hellwege, K.-H., Schäfer, K. L., Eds.; Springer-Verlag: Berlin, Germany, 1976; pp 1−129.
(16) Mori, H.; Terano, M. *Trends Polym. Sci.* **1997**, *5*, 314.
(17) Zambelli, A.; Locatelli, P.; Bajo, G.; Bovey, F. A. *Macromolecules* **1975**, *8*, 687.
(18) Sohilling, F. C.; Tonelli, A. E. *Macromolecules* **1980**, *13*, 270.
(19) Carman, C. J.; Harrington, R. A.; Wilkes, C. E. *Macromolecules* **1977**, *10*, 536.
(20) Ray, G. J.; Johnson, P. E.; Knox, J. R. *Macromolecules* **1977**, *10*, 773.
(21) Inoue, M. *J. Polym. Sci., Part A: Polym. Chem. Ed.* **1963**, *1*, 2697.
(22) Strobl, G. R. Metastable Partially Crystalline States. In *The Physics of Polymers*, 2nd ed.; Springer-Verlag: Heidelberg, Germany, 1997; pp 143−190.
(23) Quirk, R. P.; Alsamarraie, M. A. A. Physical Constants of Poly(propylene). In *Polymer Handbook*, 3rd ed.; Brandrup, J., Immergut, E. H., Eds.; John Wiley & Sons: New York, 1989; p V/27.

(24) Natta, G.; Pasquon, I. *Adv. Catal.* **1959**, *11*, 1.
(25) Keii, T.; Suzuki, E.; Tamura, M.; Doi, Y. *Makromol. Chem. Phys.* **1982**, *183*, 2285.
(26) Giannini, U. *Makromol. Chem. Suppl.* **1981**, *5*, 216.
(27) Goodall, B. L. Polypropylene: Catalysts and Polymerization Aspects. In *Polypropylene and Other Polyolefins*; Ven, S. V. D., Ed.; Elsevier: Amsterdam, 1990; pp 1−133.
(28) Kissin, Y. V. Kinetics of Olefin Polymerization with Heterogeneous Ziegler−Natta Catalysts. In *Isospecific Polymerization of Olefins*; Springer-Verlag: New York, 1985; pp 14−15.
(29) Ewen, J. A.; Elder, M. J.; Jones, R. L.; Curtis, S.; Cheng, H. N. Syndiospecific Propylene Polymerizations with *i*-Pr[CpFlu]-$ZrCl_2$. In *Catalytic Olefin Polymerization*; Keii, T., Soga, K., Eds.; Kodansha: Tokyo, 1990; pp 439−482.
(30) Busico, V.; Cipullo, R. *J. Am. Chem. Soc.* **1994**, *116*, 9329.
(31) Leclerc, M. K.; Brintzinger, H. H. *J. Am. Chem. Soc.* **1995**, *117*, 1651.
(32) Resconi, L.; Fait, A.; Piemontesi, F.; Colonnesi, M.; Rychlicki, H.; Zeigler, R. *Macromolecules* **1995**, *28*, 6667.
(33) Busico, V.; Caporaso, L.; Cipullo, R.; Landriani, L. *J. Am. Chem. Soc.* **1996**, *118*, 2105.
(34) Busico, V.; Cipullo, R.; Talarico, G.; Segre, A. L.; Chadwick, J. C. *Macromolecules* **1997**, *30*, 4786.
(35) Schneider, M. J.; Kaji, E.; Uozumi, T.; Soga, K. *Macromol. Chem. Phys.* **1997**, *198*, 2899.
(36) Plazek, D. L.; Plazek, D. J. *Macromolecules* **1983**, *16*, 1469.
(37) Pearson, D. S.; Fetters, L. J.; Younghouse, L. B.; Mays, J. W. *Macromolecules* **1988**, *21*, 478.
(38) The fractionation of the resulting block copolymer was conducted using temperature rising elution fractionation into six fractions based on the difference in the isospecificity of the PP part. Each fraction eluted at a different temperature was analyzed by ^{13}C NMR. All fractions showed peaks arising from PE-*co*-PP, indicating that the existence of the PP homopolymer could not be detected in the experiment. The detailed results will be reported in a forthcoming paper. Thus, it is considered that the formation of PP homopolymer by chain termination prior to ethene addition can scarcely occur under these conditions.
(39) Under the condition, the possibility of the existence of semicrystalline PE-*co*-PP in the insoluble fraction cannot be denied. However, a small amount of the PP-*b*-(PE-*co*-PP) having a PP part with lower stereospecificity and a shorter chain length, in addition to amorphous PE-*co*-PP, is soluble in heptane even at room temperature. On the basis of this result, the fractionation of the resulting PP-*b*-(PE-*co*-PP) was conducted with heptane at room temperature for 24 h (the amounts used were close to that of amorphous PE-*co*-PP).
(40) Wild, L. *Adv. Polym. Sci.* **1990**, *98*, 1.
(41) It must be noted that the fraction eluted at 0−45 °C was not pure amorphous PE-*co*-PP, because the PP-*b*-(PE-*co*-PP) having a PP part with lower stereospecificity and a shorter chain length is soluble in o-dichlorobenzene even below 30 °C. This consideration was supported by the results of the ^{13}C NMR analysis of the fraction of PP-*b*-(PE-*co*-PP) eluted below 30 °C and the comparison of the molecular weight between the PP homopolymer and PP-*b*-(PE-*co*-PP). Thus, we considered that the amount of the soluble fraction, which was determined by measuring the extraction with heptane at room temperature for 24 h, as shown in Table 4, is closer to that of pure amorphous PE-*co*-PP.
(42) Gedde, U. W. Microscopy of Polymers. In *Polymer Physics*; Chapman & Hall: London, 1995; pp 239−257.
(43) Olley, R. H.; Bassett, D. C. *Polymer* **1989**, *30*, 399.
(44) Bassett, D. C.; Olley, R. H. *Polymer* **1984**, *24*, 935.
(45) Mandelkern, L. The Structure of Polymers Crystallized in the Bulk. In *Crystallization of Polymers*; Kluwer Academic Publishers: Netherlands, 1993; pp 25−37.
(46) In order for successful block formation, the catalyst must behave as a living polymerization catalyst during the residence time of the polymerization, at which each active site produces only one polymer chain. Thus, improvement in the productivity is required to achieve economical feasibility. Several attempts were made directed toward commercial production, the results of which will be reported in a forthcoming paper.

MA981862B